Heliyon 9 (2023) e13170

Contents lists available at ScienceDirect

Heliyon

journal homepage: www.cell.com/heliyon

Research article

p15^{INK4B} is an alternative marker of senescent tumor cells in colorectal cancer

Soon Sang Park [a,b,c,1], Young-Kyoung Lee [a,c,1], So Hyun Park [c,d], Su Bin Lim [a,b,c], Yong Won Choi [c,e], Jun Sang Shin [f], Young Hwa Kim [c], Jang-Hee Kim [c,d,**], Tae Jun Park [a,b,c,*]

[a] Department of Biochemistry and Molecular Biology, Ajou University School of Medicine, Suwon, 16499, South Korea
[b] Department of Biomedical Sciences, Ajou University Graduate School of Medicine, Suwon, 16499, South Korea
[c] Inflamm-Aging Translational Research Center, Ajou University Medical Center, Suwon, 16499, South Korea
[d] Department of Pathology, Ajou University School of Medicine, Suwon, 16499, South Korea
[e] Department of Hematology and Oncology, Ajou University School of Medicine, Suwon, 16499, South Korea
[f] Department of Surgery, Ajou University School of Medicine, Suwon, 16499, South Korea

ARTICLE INFO

Keywords:
Cellular senescence
Senescent tumor cells
Senescence marker
p16^{INK4A}
p15^{INK4B}
Colorectal cancer

ABSTRACT

Senescent tumor cells are nonproliferating tumor cells which are closely related to cancer progression by secreting senescence-related molecules, called senescence-associated secreting phenotypes. Therefore, the presence of senescent tumor cells is considered a prognostic factor in various cancer types. Although senescence-associated β-galactosidase staining is considered the best marker for detection of senescent tumor cells, it can only be performed in fresh-frozen tissues. p16^{INK4A}, a cyclin-dependent inhibitor, has been used as an alternative marker to detect senescent tumor cells in formalin-fixed paraffin-embedded tissues. However, other reliable markers to detect senescent tumor cells is still lacking. In the present study, using public single-cell RNA-sequencing data, we found that p15^{INK4B}, a cyclin-dependent kinase inhibitor, is a novel marker for detection of senescent tumor cells. Moreover, p15^{INK4B} expression was positively correlated with that of p16^{INK4A} in colorectal cancer tissues. In *in vitro* studies, mRNA expression of p15^{INK4B} was increased together with that of p16^{INK4A} in H_2O_2- and therapy-induced cancer senescence models. However, the mRNA level of p15^{INK4B} did not increase in the oncogene-induced senescence model in primary colonic epithelial cells. In conclusion, p15^{INK4B} is a potential alternative marker for detection of senescent tumor cells together with conventional markers in advanced stages of colorectal cancer.

Abbreviations: CDK, cyclin dependent kinase; CRC, colorectal cancer; FBS, fetal bovine serum; FFPE, formalin-fixed paraffin-embedded; GSEA, gene set enrichent analysis; H3K9me3, histone H3 lysine 9 trimethylation; IHC, immunohistochemistry; SA-β-Gal, senescence-associated β-galactosidase; scRNA-seq, single cell RNA sequencing; STC, senescent tumor cell.

* Corresponding author. Department of Biochemistry and Molecular Biology, Ajou University School of Medicine, Suwon, 16499 South Korea.
** Corresponding author. Department of Pathology, Ajou University School of Medicine, Suwon, 16499 South Korea.
E-mail addresses: drjhk@ajou.ac.kr (J.-H. Kim), park64@ajou.ac.kr (T.J. Park).
[1] These authors contributed equally and shared first authorship.

https://doi.org/10.1016/j.heliyon.2023.e13170
Received 29 October 2022; Received in revised form 10 January 2023; Accepted 19 January 2023
Available online 24 January 2023

1. Introduction

Senescent tumor cells (STCs) are present in a variety of cancer types [1–6]. STCs play distinct roles in cancer progression from that of non-STCs [2–5]. Growth arrest is an important feature of senescent cells [7,8], but secretion of multiple cytokines and/or chemokines related to cancer invasion and immune evasion are markedly increased in STCs [3,9]. Furthermore, STCs vigorously secrete proteins that can break down the extracellular matrix, such as matrix metalloproteinases [2]. Therefore, the presence of STCs is considered a poor prognostic factor in various cancer types [10–12]. However, identifying STCs within cancer tissue has many potential limitations. Senescence-specific morphologic changes *in vitro*, such as increased cell size, vacuole number, and heterochromatin foci [13], are difficult to observe *in vivo* [1]. Therefore, at present, senescence-associated β-galactosidase (SA-β-Gal) staining has been considered the best marker for detection of STCs, including *in vitro* and *in vivo* systems [1–3,14]. However, SA-β-Gal staining cannot be performed in formalin-fixed paraffin-embedded (FFPE) tissue, as β-galactosidase activity cannot be maintained in paraffin-embedded samples [1]. Therefore, only fresh-frozen tissues can be used to perform SA-β-Gal staining [1,14]. To overcome this limitation, $p16^{INK4A}$ has emerged as an alternative immunohistochemistry (IHC) marker to replace SA-β-Gal staining to detect STCs in FFPE tissues [2,3]. $p16^{INK4A}$, a representative cyclin-dependent kinase (CDK) 4/6 inhibitor, is a powerful molecule that can easily induce cell cycle arrest [15]. Therefore, $p16^{INK4A}$ has been widely used as a senescence marker for *in vitro* and *in vivo* models, including cancer tissues [16–18]. In our previous studies, we observed that expression of $p16^{INK4A}$ strongly correlated with SA-β-Gal staining in papillary thyroid cancer and colorectal cancer (CRC) [2,3]. These results suggest that $p16^{INK4A}$ can be used as a reliable senescence marker when fresh tissues cannot be obtained for SA-β-Gal staining. However, $p16^{INK4A}$ IHC analysis also has several limitations. Because $p16^{INK4A}$ is a tumor suppressor gene, it is subject to mutation, and mutated forms of $p16^{INK4A}$ are frequently detected in cancer tissue[19–21]. Also, HPV infection, the most common pathological driver of cervical cancer, can induce overexpression of the viral proteins E6 and E7 [22], and $p16^{INK4A}$ can be also overexpressed as part of a negative feedback loop [23], leading to false positivity of these samples. Therefore, considering the lack of a definitive senescence marker in paraffin-embedded samples, cellular senescence is often verified using multiple markers, such as $p21^{Waf1}$ and p53 [24,25]. Although $p21^{Waf1}$ and p53 are good senescence markers for normal cells [25–27], they are not adequate markers for STCs, as they are frequently mutated in multiple cancer types [28–31] and do not correlate with SA-β-Gal staining [3]. Although histone H3 lysine 9 trimethylation (H3K9me3), heterochromatin-related epigenetic change of senescent cells, is weakly correlated with SA-β-Gal staining [3,32], H3K9me3 is less specific than $p16^{INK4A}$. In the present study, we used public single-cell RNA-sequencing (scRNA-seq) data to identify that $p15^{INK4B}$, another CDK inhibitor, is a novel marker for STCs in CRC. Further, IHC analysis revealed that $p15^{INK4B}$ expression was highly correlated with $p16^{INK4A}$ in FFPE CRC tissues. Therefore, $p15^{INK4B}$ can be considered as an alternative marker to replace $p16^{INK4A}$ for detection of STCs in CRC.

2. Materials and methods

2.1. Patient CRC samples

After informed consent, CRC samples were obtained from patients at Ajou University Hospital following surgical resection. The study was approved by the Institutional Review Board of Ajou University Hospital (AJOUIRB-OBS-2016-218) and was conducted in accordance with the Declaration of Helsinki. Fresh tumor tissue was sampled by an experienced pathologist (J.-H. K.) immediately after resection and separated into two portions. One portion was used to generate frozen tissue using liquid nitrogen snap-freezing, and the second portion was processed for FFPE. To reduce potential bias caused by genetic background, only CRC patients without microsatellite instability were selected. Patients who received neoadjuvant chemotherapy or radiation therapy were also excluded.

2.2. IHC analysis

CRC tissue section review was performed independently by an experienced pathologist (J.-H. K.). A section of cut edge from fresh-frozen tissue was used for SA-β-Gal staining. The other section of cut edge from FFPE tissue was used for IHC analysis. IHC analysis was performed using a Benchmark XT automated processor (Ventana Medical Systems Inc, Tucson, AZ) on 4-μm-thick tissue sections of FFPE blocks. The following primary antibodies were used: $p16^{INK4A}$, predilution (805–4713, Roche, Tucson, AZ); $p15^{INK4B}$, 1:700 (SAB4500078, Sigma-Aldrich, Burlington, MA); $p21^{Waf1}$, 1:300 (2990-1, Epitomics, Burlingame, CA); $p27^{Kip1}$, 1:100 (NB110-66664, Novus Biologicals, Littleton, CO); p53, predilution (805–4713, Roche, Tucson, AZ); and $p14^{ARF}$, 1:200 (74560, Cell Signaling Technology, Danvers, MA).

2.3. Lentivirus preparation

Lentiviral particles were prepared by co-transfecting a lentiviral expression vector containing $BRAF^{V600E}$ mutation with lentiviral packaging plasmids (pGagpol, pVSV-G) to HEK-293TN cells. The supernatant was harvested after 48 h.

2.4. Cell culture and induction of senescence

The CRC cell line SW480 was purchased (CCL-228, ATCC, Manassas, VA). SW480 was maintained in complete RPMI media (LM011-60, Welgene, Gyeongsan, Korea) with 10% fetal bovine serum (FBS) (16000044, Gibco, Billings, MT) and 1% antibiotic-antimycotic solution (15240062, Gibco, Billings, MT). To establish the H_2O_2 and doxorubicin-induced senescence model, 1.5×10^5

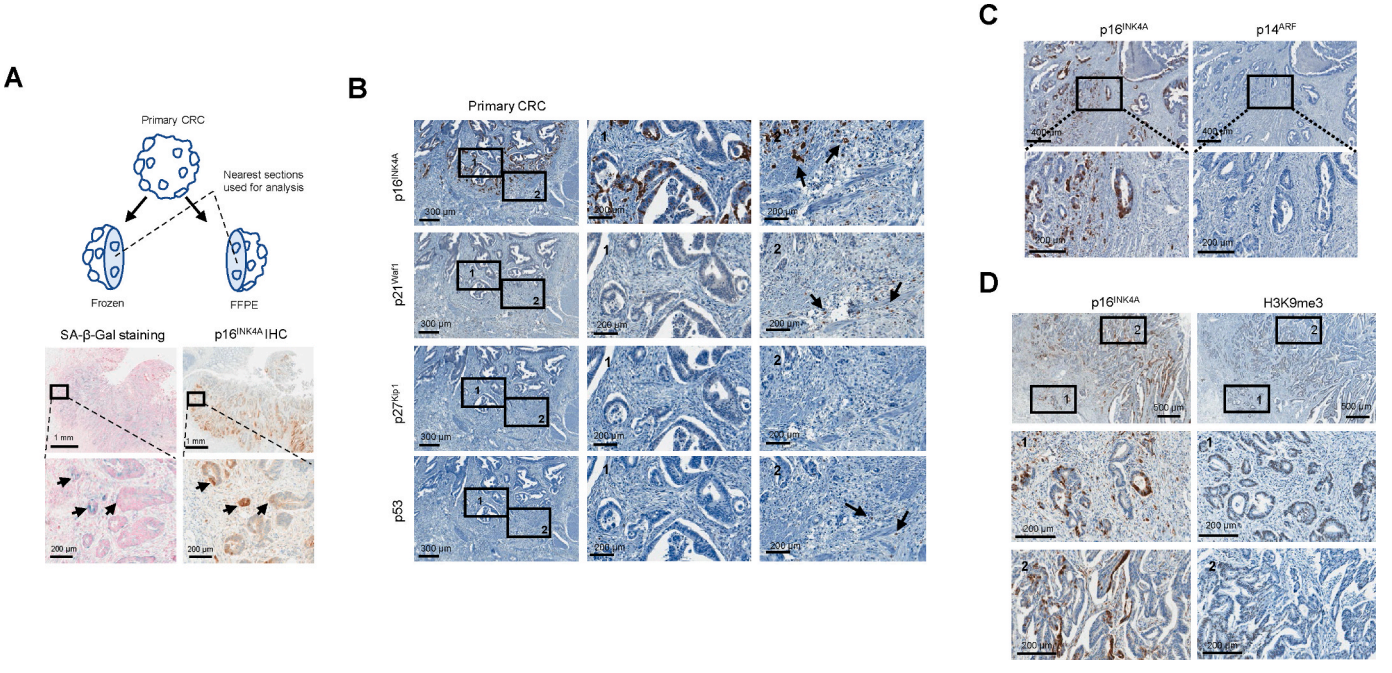

Fig. 1. Conventional senescence markers for detection of STCs in CRC. (A) A surgically removed fresh CRC tissue was cut into two segments. One segment was frozen and used for SA-β-Gal staining, and the other segment was processed for FFPE to perform IHC analysis. The nearest sections from frozen tissue (for SA-β-Gal staining, left) and FFPE tissue (for IHC $p16^{INK4A}$ staining, right) were used for analysis. Arrows indicate SA-β-Gal positive cells. **(B)** IHC analysis with the conventional senescence markers $p21^{Waf1}$, $p27^{Kip1}$, and p53, is shown. **(C)** Serial sections of CRC tissue were stained with $p16^{INK4A}$ and H3K9me3. Arrows indicate immune-like cells which are positive for $p21^{Waf1}$or p53.

SW480 cells were seeded into 60 mm culture-treated dishes (353002, Falcon, New York, NY). One day after seeding, cells were treated with 60 μM H_2O_2 (H1009, Sigma-Aldrich, Burlington, MA) or 50 nM doxorubicin (Adriamycin-RDF Injection, Ildong Pharmaceutical, Seoul, Korea) and incubated for 48 h. Subsequently, media was replaced with fresh media, and cells were stained or analyzed after stabilization (48 h). To check heterochromatin foci in senescence models, 1:10,000 diluted DAPI solution (ab228549, Abcam, Cambridge, UK) was stained and cells were observed under fluorescence microscopy (AXIO Imager.M1, Zeiss, Oberkochen, Germany). Human dermal fibroblasts were isolated from the foreskin. Fibroblasts at passage 3–7 were maintained in Dulbecco's modified Eagles Medium (LM011-02, Welgene, Gyeongsan, Korea) supplemented with 10% FBS. Primary human colon epithelial cells (2950, ScienCell Research Laboratories, Carlsbad, CA) were maintained in the colonic epithelial cell medium (2951, ScienCell Research Laboratories, Carlsbad, CA). To induce an oncogene-induced senescence (OIS) model, primary colon epithelial cells and human dermal fibroblasts were infected with lentiviruses harboring $BRAF^{V600E}$ for 5 days.

2.5. SA-β-Gal staining

Slides from the frozen tissue were fixed with 10% paraformaldehyde (30525-89-4, Sigma-Aldrich, Burlington, MA) for 1 min and incubated with SA-β-Gal solution [1 mg/mL X-gal (X4281C, Goldbio, Saint Louis, MO), 40 μM citric acid monohydrate (1287, Duksan, Seoul, Korea, pH 5.8); 5 μM potassium ferrocyanide (P3289, Sigma-Aldrich, Burlington, MA); 5 μM potassium ferricyanide (702587, Sigma-Aldrich, Burlington, MA); 150 μM sodium chloride (81, Duksan, Seoul, Korea); 2 μM $MgCl_2$ (M8266, Sigma-Aldrich, Burlington, MA)] for 12 h in 37 °C incubator. Cultured cells were fixed with 4% paraformaldehyde and incubated with SA-β-Gal solution. After washing cells with phosphate buffered saline, SA-β-Gal-positive cells were analyzed under light microscopy.

2.6. Real-time polymerase chain reaction (RT-PCR)

First-strand cDNA was synthesized using the SuperScript IV First-Strand Synthesis System (18091200, Invitrogen, Carlsbad, CA) from 1 μg total cellular RNA. Real-time PCR was conducted with SYBR Green PCR Master Mix (#1708880, Bio-Rad, Hercules, CA) under the following conditions: initial activation at 95 °C for 5 min, 50 cycles of 95 °C for 15 s, and 60 °C for 1 min. Primers used for real-time PCR were as follows: $p16^{INK4A}$: 5'-CAT CAT GAC CTG GAT CGG C-3' and 5'-GGG TCG GGT AGA GGA GGT G-3'; $p15^{INK4B}$: 5' -GAC CGG GAA TAA CCT TCC AT- 3' and 5'- CAC CAG GTC CAG TCA AGG AT-3'; β-Actin: 5' –CCC TGG CAC CCA GCA C- 3' and 5' -GCC GAT CCA CAC GGA GTA C- 3'; BRAF: 5' -AGA AAG CAC TGA TGA TGA GAG G- 3' and 5' -GGA AAT ATC AGT GTC CCA ACC A-3'.

2.7. scRNA-seq analysis of a public dataset

A public CRC scRNA-seq dataset (GSE166555) was used for analysis [33]. Analysis was performed using the R (v 4.0.3) "Seurat" package (v 4.0.1) [34]. Among the twelve patients in this dataset, six patients (#7, #8, #17, #20, #21, and #25) with microsatellite-stable status and conventional inferred progression, and for whom both normal and tumor tissue samples were available, were included in analyses [33]. To gather cell singlets, cells expressing the number of featured gene >200 and <10,000 were selected. Cells containing more than 50% mitochondrial DNA were previously excluded. To decide the appropriate number of dimensions for principal component analysis (PCA), Jackstraw scores were calculated using 'ScoreJackStraw' function of the "Seurat" package, and 20 dimensions were appropriate for further analysis ($p < 0.001$). Cells with read counts of *EPCAM* > 1 and *CDX2* > 1 were annotated as cancer cells, and cancer cells with *CDKN2A* read count >0 were annotated as *CDKN2A*-positive STCs. To exclude the interpatient variance and batch effect, a detailed analysis was performed on patient #8, which markedly expressed *CDKN2A* [33]. To re-cluster the cells from patient #8, jackstraw scores were calculated, and three dimensions were appropriate for subsequent PCA ($p < 0.001$). To discover markers for *CDKN2A*-positive cancer cells, 'FindMarkers' function from Seurat package using Wilcoxon rank sum test was used [34]. Gene set enrichment analysis (GSEA) was performed using the "fgsea" package in R (v 4.0.3) [35]. Permutations were performed 1,000 times, and *p* values were calculated using statistics from GSEA [36]. The weighted Kolmogorov-Smirnov statistics were calculated as the running sum of a ranked gene list [36]. Benjamin Hochberg (BH)-adjusted *p* values were also calculated, and values < 0.01 were considered statistically significant.

2.8. Statistical analysis

The statistical differences of the mean values between two groups were evaluated using a Student's *t*-test. The median values between two groups were compared using a Mann-Whitney *U* test. The statistical differences of the proportions between two groups were assessed using Chi-square test or Fisher's exact test.

3. Results

3.1. Conventional senescence markers for detection of STCs in CRC

To evaluate the specificity of $p16^{INK4A}$ as an appropriate marker for STCs, a fresh CRC mass was cut into two pieces immediately following surgical resection, and the separate pieces were processed into frozen tissue or a paraffin block (Fig. 1A). When a section from a paraffin block was stained with $p16^{INK4A}$, the $p16^{INK4A}$-positive area in FFPE tissue overlapped with that of SA-β-Gal staining

from the frozen tissue (Fig. 1A). These results indicated that $p16^{INK4A}$ was a reliable marker for STCs. However, serial staining of $p16^{INK4A}$, $p21^{Waf1}$, $p27^{Kip1}$, and p53 revealed that IHC results of $p21^{Waf1}$, $p27^{Kip1}$, and p53 were substantially differed from that of $p16^{INK4A}$ (Fig. 1B); $p21^{Waf1}$ and p53 mostly stained peritumoral round-shaped immune-like cells rather than cancer epithelial cells, and $p27^{Kip1}$ did not stain any cell in CRC tissues (Fig. 1B). Moreover, expression pattern of another transcript variant of *CDKN2A* gene, $p14^{ARF}$, was totally different from that of $p16^{INK4A}$ which implies a major translated form of *CDKN2A* gene is $p16^{INK4A}$ in CRC (Fig. 1C). Although H3K9me3 IHC results exhibited a weak positive correlation with that of $p16^{INK4A}$, nonspecific false-positive cancer cells were frequently detected (Fig. 1D).

3.2. $p15^{INK4B}$ is an alternative marker for detection of STCs in CRC in vivo

scRNA-seq analysis using the public dataset GSE166555 was performed to identify alternative markers for STCs [33]. From six patients, 13,701 cells were analyzed, and cells from patient #8, who prominently expressed *CDKN2A* were used for further analysis to minimize the inter-patient variance and batch effect (Fig. S1A and S1B). Subsequently, 274 cancer cells from patient #8 were re-clustered to confirm whether CDKN2A-positive cells had a unique gene expression pattern and clustered together (Fig. S1B and 2A). Interestingly, most *CDKN2A*-positive cancer cells were clustered together in cluster 1, suggesting *CDKN2A*-positive cells have similar gene expression patterns (Fig. 2A). In addition, cells from cluster 1 did not express the proliferation marker *MKI67*, suggesting that the cell cycle was arrested (Fig. 2A and B). To confirm that the cells from cluster 1 showed a senescence phenotype, GSEA was performed in multiple gene sets, which revealed that cells from cluster 1 highly expressed senescence-related genes (Table 1 and Fig. 2C). Moreover, $p15^{INK4B}$ (*CDKN2B*) was one of the top markers among the leading edges of the GSEA along with $p16^{INK4A}$ (*CDKN2A*) in the oxidative stress-induced senescence gene set (ES = 0.408, NES = 3.52, adjusted *p* value = 0.0042) (Fig. 2C). The dot plot showed that cluster 1 highly expressed *CDKN2A* and *CDKN2B* (Fig. 2D). To confirm whether the gene expression features of cluster 1 were derived from *CDKN2A*-positive cells, the cells were exclusively extracted and compared to *CDKN2A*-negative cells (Fig. S2A). Similar with the gene expression of the cluster 1, *CDKN2A*-positive cells were negative for *MKI67* (Fig. S2A). In addition, *CDKN2B* was one of the top markers representing *CDKN2A*-positive cells (Fig. S2B). The dot plot also revealed that cells expressing *CDKN2A* specifically expressed *CDKN2B,* another type of tumor suppressor (Fig. S2C). GSEA also confirmed that senescence-related genes were significantly upregulated in *CDKN2A*-positive cells (ES = 0.354, NES = 3.04, adjusted *p* value = 0.0061), and *CDKN2B* was the top gene among the leading edges (Fig. S2D). To check protein expression of $p15^{INK4B}$ in STCs, IHC analysis of $p15^{INK4B}$ was performed with a conventional marker, $p16^{INK4A}$, using serial sections. The $p15^{INK4B}$ expression patterns were highly correlated with the $p16^{INK4A}$ expression patterns (Fig. 2E). Contrastingly, $p15^{INK4B}$ IHC results were also negative in $p16^{INK4A}$-negative CRC patients (Fig. 2F). Subsequently, $p15^{INK4B}$ expression patterns of 21 total cases [$p16^{INK4A}$-negative patients (n = 7) *vs.* $p16^{INK4A}$-positive patients (n = 14)] were analyzed and revealed that the expression patterns of $p15^{INK4B}$ were same with that of $p16^{INK4A}$ (Table 2 and Fig. 2G). These results demonstrated that $p15^{INK4B}$, together with $p16^{INK4A}$, can be used as a reliable STC marker.

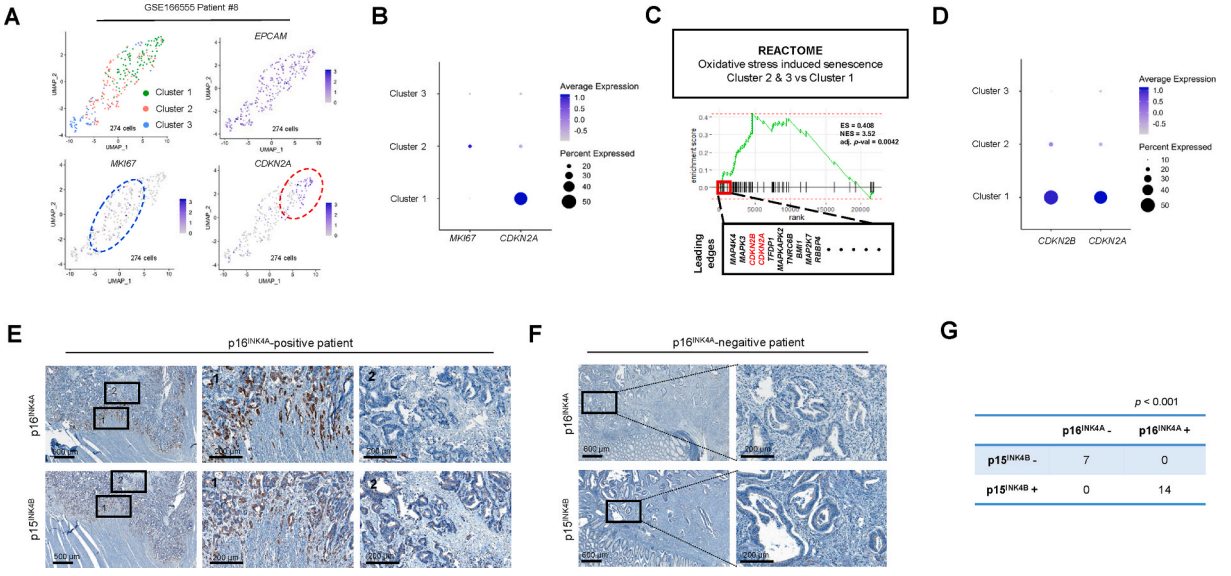

Fig. 2. $p15^{INK4B}$ is an alternative marker for detection of STCs in CRC *in vivo*. **(A)** Clusters of *EPCAM*-positive cancer cells from patient #8 and feature plots of *MKI67* and *CDKN2A*. **(B)** Dot plot showing the expression pattern of the senescence marker *CDKN2A* and the proliferation marker *MKI67* in each cluster. **(C)** GSEA using a cellular senescence-related gene set. Leading edges which are upregulated in cluster 1 are shown in the box below. **(D)** Dot plot showing the expression pattern of *CDKN2A* and *CDKN2B* in each cluster. **(E)** IHC analysis using serial sections from $p16^{INK4A}$-positive FFPE CRC tissue. **(F)** IHC analysis using serial sections from $p16^{INK4A}$-negative FFPE CRC tissue. **(G)** Table showing correlations between $p15^{INK4B}$ and $p16^{INK4A}$ expression in FFPE IHC samples. The *p* value was calculated using Fisher's exact test.

Table 1
Senescence-related pathways in the cluster 1 based on GSEA.

Pathway	*p* value	Adj. *p*-val	ES	NES
GOBP_CELLULAR_SENESCENCE (Geneset number: GO0090398)	0.0014[a]	0.0081[b]	0.32	2.90
REACTOME_CELLULAR_SENESCENCE (Geneset source: Pubmed18711403) [37]	0.0013[a]	0.0050[b]	0.38	4.35
REACTOME_OXIDATIVE_STRESS_INDUCED _SENESCENCE (Geneset source: NA)	0.0014[a]	0.0050[b]	0.41	3.45
FRIDMAN_SENESCENCE_UP (Geneset source: Pubmed18711403) [37]	0.0014[a]	0.0050[b]	0.33	2.98
REACTOME_SENESCENCE_ASSOCIATED _SECRETORY_PHENOTYPE_SASP (Geneset source: NA)	0.0015 a	0.0050[b]	0.35	2.77
REACTOME_ONCOGENE_INDUCED_SENESCENCE (Geneset source: NA)	0.0015[a]	0.0050[b]	0.42	2.71

[a] *p* values were obtained from 1000 times permutation.
[b] *p* values were obtained from Benjamin Hochberg adjustment of *p* values. Adj. *p* val, adjusted *p* value; ES, enrichment score; NA, not applicable; NES, normalized enrichment score.

Table 2
Patient characteristics according to their $p16^{INK4A}$ expression in IHC analysis.

	Total (n = 21)	$p16^{INK4A}$-negative (n = 7)	$p16^{INK4A}$-positive (n = 14)	*p* value
Age, median	66.00	70.00	61.00	0.062[a]
Male, n (%)	12 (57.14)	5 (71.43)	7 (50.00)	0.64[b]
T staging, n (%)				0.13[b]
1	0 (0)	0 (0)	0 (0)	
2	1 (4.76)	0 (0)	1 (7.14)	
3	19 (90.48)	6 (85.71)	13 (92.86)	
4	1 (4.76)	1 (14.29)	0 (0)	
N staging, n (%)				0.85[b]
0	8 (38.10)	3 (42.86)	5 (35.71)	
1	6 (28.57)	1 (14.29)	5 (35.71)	
2	7 (33.33)	3 (42.86)	4 (28.57)	
M staging, n (%)				1.00[b]
0	21 (100)	7 (100)	14 (100)	
1	0 (0)	0 (0)	0 (0)	
Localization, n (%)				0.15[b]
Ascending	0 (0)	0 (0)	0 (0)	
Transverse	1 (4.76)	1 (14.29)	0 (0)	
Descending/sigmoid/rectum	20 (95.24)	6 (85.71)	14 (100)	
Microsatellite stable, n (%)	21 (100)	7 (100)	14 (100)	1.00[b]

[a] *p* values were obtained from Mann-Whitney U test.
[b] *p* values were obtained from Chi-square test.

3.3. STC $p15^{INK4B}$ expression in vitro

In the present study, SW480, a CRC cell line, was used to establish a cancer cell senescence model. The most reliable senescence marker, SA-β-Gal staining, exhibited increased positivity both in H_2O_2-induced and doxorubicin-induced STC models (Fig. 3A). DAPI staining also showed that senescence-associated heterochromatin foci (SAHF), a senescence marker, are more frequently detected in senescent cancer cells compared to control cells in both models (Fig. 3B). Interestingly, in both models, mRNA expression of $p15^{INK4B}$ increased concomitantly with that of $p16^{INK4A}$ (Fig. 3C). Another cellular senescence model, the OIS model, was introduced by overexpressing mutated *BRAF* ($BRAF^{V600E}$) in primary colonic epithelial cells (Fig. S3A). In this model, mRNA expression level of $p16^{INK4A}$ increased after cellular senescence induction (Fig. S3B). However, $p15^{INK4B}$ expression did not show any difference (Fig. S3B). These results suggest that $p15^{INK4B}$ is a reliable marker for STCs, but a questionable one for precancerous colonic epithelial cells, such as OIS.

4. Discussion

From the perspective of cancer treatment, STC detection is important because (i) STCs secrete multiple cancer-promoting molecules and targeting STCs or their secreted molecules could inhibit cancer progression [1–3]; and (ii) STCs remain after primary treatment and are highly related to long-term cancer relapse [38,39]. Therefore, STC detection is very important for patient prognosis, although the importance of STCs in cancer progression has long been overlooked. Because conventional CDK inhibitors such as $p16^{INK4A}$, $p21^{Waf1}$, and $p27^{Kip1}$ can induce cell cycle arrest in normal cells, they have been widely used as cellular senescence markers [24,27,40]. However, CDK inhibitors also function as tumor suppressors, such that cancers must overcome the tumor-suppressing effects of CDK inhibitors for successful cancer progression [41–43]. Therefore, deletions and mutations are frequently detected in the loci of CDK inhibitors in cancer tissues, precluding the ability to detect STCs within these tissues [43]. Therefore, to our current knowledge, SA-β-Gal staining, which detects lysosomal β-galactosidase in senescent cells, is the most reliable marker for STC detection [44].

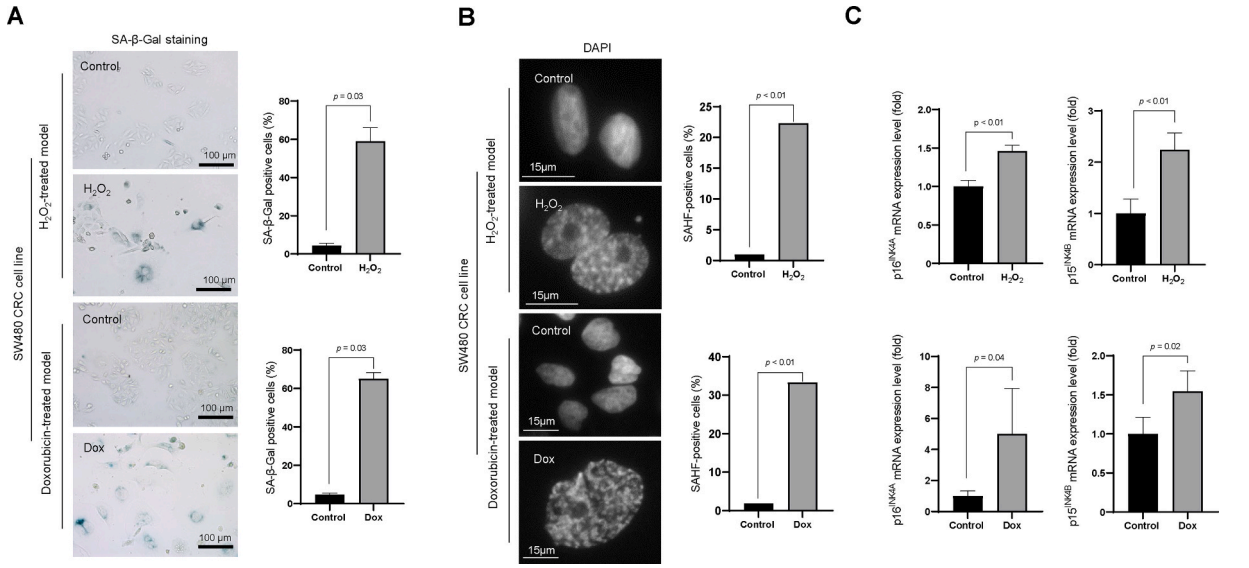

Fig. 3. STC p15^{INK4B} expression *in vitro*. **(A)** SA-β-Gal staining in two cancer cell senescence models, H_2O_2-induced (60 μM) and doxorubicin (Dox)-induced (50 nM) senescence models (n = 4, each). The *p* values are obtained using Mann-Whitney *U* test. **(B)** DAPI staining revealed heterochromatin foci, in both H_2O_2-induced (60 μM) and doxorubicin (Dox)-induced (50 nM) senescence models. The proportion of SAHF-positive cells out of total cells was shown in the bar graph and *p* values were obtained from chi-square test. **(C)** mRNA expression of *CDKN2A* and *CDKN2B* in H_2O_2-induced (60 μM) and doxorubicin (Dox)-induced (50 nM) senescence models (n = 3, each). The *p* values were obtained using Student's *t*-test.

However, SA-β-Gal staining requires fresh-frozen tissues. The major obstacle of cancer cell senescence research using fresh-frozen tissue is that a section cannot be simultaneously performed for SA-β-Gal staining and IHC analysis. Therefore, to reveal the physiological role of STCs using fresh-frozen tissue, SA-β-Gal staining and IHC analysis using serial sections should be performed. However, obtaining intact serial sections from fresh-frozen tissue is technically demanding. Moreover, even if it were to be performed, the overall morphology of frozen tissues can easily be distorted during a sectioning and staining process, and they might not be suitable for subsequent analysis. Therefore, novel markers of STCs which can be used in FFPE tissue is important, but unfortunately, for FFPE blocks, no definite markers for STC markers are currently available. Alternatively, multiple markers, including CDK inhibitors and other senescence markers such as H3K9me3, are stained simultaneously or serially to detect STCs in FFPE tissues [1,32]. Also, because the mutation patterns of CDK inhibitors vary according to cancer type [44], the preferred combination of these markers is cancer type dependent. In our previous study, we revealed that p16^{INK4A} staining is the most reliable marker to detect STCs in the CRC FFPE tissue, which was positively correlated with SA-β-Gal staining [3]. In contrast, in this study, p21^{Waf1} and p53, two additional renowned senescence markers, were not correlated with SA-β-Gal staining and p16^{INK4A} IHC analysis. A probable explanation is that not only the frequent epigenetic changes in the promoter region of p21^{Waf1} and p53 [45–47] but also frequent mutations of the genes themselves contributed to this phenotype [29–31]. Moreover, although crosstalk exists between the p53-p21^{Waf1} and p16^{INK4A}-Rb pathways [48,49], each pathway may act independently, according to the type of insult and upstream signals [48]. It is widely accepted that the p53-p21^{Waf1} pathway is induced in relatively early stages of DNA damage [50]. Therefore, induction of p53 and p21^{Waf1} is more likely to be DNA damage-dependent than senescence-dependent [50]. In contrast, p16^{INK4A} is an essential molecule that continuously maintains cellular senescence [51,52]. This implies that p16^{INK4A} is a more powerful inducer of cell cycle arrest than either p21^{Waf1} or p53 [51,52]. This is consistent with a previous report showing that although p16^{INK4A} induction can be prevented by p53 inactivation, once p16^{INK4A} is expressed, p53 downregulation could not reverse cell cycle arrest [49]. Therefore, p16^{INK4A} is a relatively more reliable marker than p53 and p21^{Waf1} to detect STCs in CRC. However, use of p16^{INK4A} as the sole marker to detect STCs in CRC is problematic as p16^{INK4A} mutations and gene silencing are commonly detected in CRC patients [53,54]. Therefore, to our knowledge, IHC analysis of p16^{INK4A}, together with H3K9me3 and Ki-67, is considered optimal for detection of STCs in CRC FFPE tissue.

Another major obstacle to identify a novel marker of STCs is uneven distribution of STCs in cancer tissues [2,3]. Because most of STCs are in the margin of the cancer tissue [2], the targeted region to collect STCs are easily contaminated by other stromal cells when bulk RNA-sequencing or microdissection-assisted RNA-sequencing are performed. To overcome this limitation, in this study, scRNA-seq analysis which can minimize the contamination issue was performed using public dataset. Consequently, we found that p15^{INK4B}, a type of CDK inhibitors, can be another marker to detect STCs in CRC. The physiologic role of p15^{INK4B} is similar to that of p16^{INK4A}, as it complexes with CDK4/6 and hinders its interaction with cyclin D, resulting finally in cell cycle arrest [55]. In fact, p15^{INK4B} has often been used as a senescence marker in previous studies [56,57]. Especially, Mirzakhani and colleagues recently reported that p15^{INK4B} expression was related with androgen-induced cellular senescence in prostate cancer cells [58]. However, as our current knowledge, this is the first study which proposed p15^{INK4B} as a STC marker comparing its expression with other conventional senescence markers in CRC.

In this study, we established an OIS model by overexpressing *BRAF*^{V600E}, an important mutation in colorectal cancer in primary

colon epithelial cells [59]. *BRAF*^{V600E}-overexpression increased p16^{INK4A} mRNA expression in colonic epithelial cells. However, p15^{INK4B} mRNA expression did not show any difference. The results are contradictory with another result using fibroblasts which showed increased p15^{INK4B} expression in same experimental condition with primary colon epithelial cells (Fig. S4A and S4B). It is consistent with the previous study performed by Kuilman and colleagues that p15^{INK4B} was induced by *BRAF*^{V600E} overexpression in human dermal fibroblasts [60]. The result might be caused by the difference in cellular origin (mesenchymal origin fibroblasts *vs.* epithelial origin colonic epithelial cells), although the exact mechanism should be elucidated. Kuilman and colleagues also showed that p15^{INK4B} expression can be suppressed by IL-6 depletion [60]. The expression level of IL-6 of colon epithelial cells is much lower than stromal cells including fibroblasts in the normal tissue [61]. Therefore, p15^{INK4B} might not have been induced due to the low level of the basal IL-6 in colonic epithelial cells of normal tissues. In addition, another explanation for this phenotype is that senescence-inducing signaling pathways of normal epithelial cells might be different from that of cancer cells in advanced stages [62]. Conclusively, p15^{INK4B} is a reliable marker for STCs, but a questionable one for OIS of precancerous colonic epithelial cells.

p15^{INK4B} also has several limitations as a marker for STCs. First, p15^{INK4B} itself is often deleted or mutated in multiple cancer tissues [63–65]. Therefore, IHC analysis can produce a false positive when *CDKN2B* is mutated. Secondly, although more *in vivo* evidence is needed, p15^{INK4B} might not detect some kinds of senescent epithelial cells such as OIS of precancerous cells as discussed above. Third, the locus for *CDKN2B* is proximal to *CDKN2A*, a gene coding p16^{INK4A}, suggesting that *CDKN2A* is subject to similar regulation processes [66]. Therefore, it is possible that regulation of genetic mutation or deletion of *CDKN2B* occurs together with that of *CDKN2A* [63]. However, although definite evidence in CRC is still lacking, *CDKN2A* and *CDKN2B* mutations or deletions are not always happen together [66–69]. Moreover, epigenetic regulation such as promoter methylation of p14^{ARF}, p15^{INK4B}, and p16^{INK4A} can be controlled separately [69], which implies that p15^{INK4B} is still a potential marker of STCs despite of several limitations. Therefore, p15^{INK4B} is an excellent alternative option when false-positive p16^{INK4A} FFPE IHC results are highly suspected.

5. Conclusions

In conclusion, integrative analysis of scRNA-seq data, *in vivo* IHC analysis, and *in vitro* experiments revealed that p15^{INK4B} is an appropriate marker for STCs in CRC. Therefore, p15^{INK4B} is one of a few markers that can reliably detect STCs in FFPE CRC samples.

Declarations

Author contribution statement

Soon Sang Park; Young-Kyoung Lee: Performed the experiments; Analyzed and interpreted the data; Wrote the paper.
So Hyun Park: Performed the experiments.
Su Bin Lim: Analyzed and interpreted the data; Contributed reagents, materials, analysis tools or data.
Yong Won Choi: Analyzed and interpreted the data.
Jun Sang Shin: Contributed reagents, materials, analysis tools or data.
Young Hwa Kim: Performed the experiments; Contributed reagents, materials, analysis tools or data.
Jang-Hee Kim: Conceived and designed the experiments; Performed the experiments; Analyzed and interpreted the data.
Tae Jun Park: Conceived and designed the experiments; Wrote the paper.

Funding statement

Tae Jun Park was supported by National Research Foundation of Korea [NRF-2019R1A2C2086127; NRF-2020R1A6A1A03043539; NRF-2020M3A9D8037604].

Young-Kyoung Lee was supported by National Research Foundation of Korea [NRF-2020R1C1C1007611].

Soon Sang Park was supported by a grant of the MD-Phd/Medical Scientist Training Program through the Korea Health Industry Development Institute (KHIDI), funded by the Ministry of Health and Welfare, Republic of Korea.

Data availability statement

Data associated with this study has been deposited at NCBI gene expression omnibus under the accession number GSE166555.

Declaration of interest's statement

The authors declare no competing interests.

Appendix A. Supplementary data

Supplementary data related to this article can be found at https://doi.org/10.1016/j.heliyon.2023.e13170.

References

[1] S.S. Park, Y.W. Choi, J.H. Kim, et al., Senescent tumor cells: an overlooked adversary in the battle against cancer, Exp. Mol. Med. 53 (12) (2021) 1834–1841, https://doi.org/10.1038/s12276-021-00717-5.

[2] Y.H. Kim, Y.W. Choi, J. Lee, E.Y. Soh, J.H. Kim, Senescent tumor cells lead the collective invasion in thyroid cancer, Nat. Commun. 8 (1) (2017) 1–14, https://doi.org/10.1038/ncomms15208.

[3] Y.W. Choi, Y.H. Kim, S.Y. Oh, et al., Senescent tumor cells build a cytokine shield in colorectal cancer, Adv. Sci. 8 (4) (2021), 2002497, https://doi.org/10.1002/advs.202002497.

[4] M. Karabicici, S. Alptekin, F.Z. Firtina Karagonlar, E. Erdal, Doxorubicin-induced senescence promotes stemness and tumorigenicity in EpCAM-/CD133-nonstem cell population in hepatocellular carcinoma cell line, HuH-7, Mol. Oncol. 15 (8) (2021) 2185–2202, https://doi.org/10.1002/1878-0261.12916.

[5] M. Milanovic, N.D. Fan, D. Belenki, et al., Senescence-associated reprogramming promotes cancer stemness, Nature 553 (7686) (2018) 96–100, https://doi.org/10.1038/nature25167.

[6] Y.H. Kim, T.J. Park, Cellular senescence in cancer, BMB Reports 52 (1) (2019) 42, https://doi.org/10.5483/BMBRep.2019.52.1.295.

[7] L. Hayflick, S.P. Moorhead, The serial cultivation of human diploid cell strains, Exp. Cell Res. 25 (3) (1961) 585–621, https://doi.org/10.1016/0014-4827(61)90192-6.

[8] R. Di Micco, V. Krizhanovsky, D. Baker, F. d'Adda di, Cellular senescence in ageing: from mechanisms to therapeutic opportunities, Nat. Rev. Mol. Cell Biol. 22 (2) (2021) 75–95, https://doi.org/10.1038/s41580-020-00314-w.

[9] J.P. Coppé, P.Y. Desprez, A. Krtolica, J. Campisi, The senescence-associated secretory phenotype: the dark side of tumor suppression, Annu. Rev. Pathol. 5 (2010) 99–118, https://doi.org/10.1146/annurev-pathol-121808-102144.

[10] L. Wang, L. Lankhorst, R. Bernards, Exploiting senescence for the treatment of cancer, Nat. Rev. Cancer 22 (6) (2022) 340–355, https://doi.org/10.1038/s41568-022-00450-9.

[11] B. Wang, J. Kohli, M. Demaria, Senescent cells in cancer therapy: friends or foes? Trends Canc. 6 (10) (2020) 838–857, https://doi.org/10.1016/j.trecan.2020.05.004.

[12] L. Wyld, I. Bellantuono, T. Tchkonia, et al., Senescence and cancer: a review of clinical implications of senescence and senotherapies, Cancers 12 (8) (2020) 2134, https://doi.org/10.3390/cancers12082134.

[13] A. Hernandez-Segura, J. Nehme M. Demaria, Hallmarks of cellular senescence, Trends Cell Biol. 28 (6) (2018) 436–453, https://doi.org/10.1016/j.tcb.2018.02.001.

[14] G.P. Dimri, X. Lee, G. Basile, et al., A biomarker that identifies senescent human cells in culture and in aging skin in vivo, Proc. Natl. Acad. Sci. U.S.A. 92 (20) (1995) 9363–9367, https://doi.org/10.1073/pnas.92.20.9363.

[15] J.L. Bruce, R.K. Hurford Jr., M. Classon, J. Koh, N. Dyson, Requirements for cell cycle arrest by p16INK4a, Mol. Cell 6 (3) (2000) 737–742, https://doi.org/10.1016/S1097-2765(00)00072-1.

[16] A.J. Brenner, M.R. Stampfer, C.M. Aldaz, Increased p16 expression with first senescence arrest in human mammary epithelial cells and extended growth capacity with p16 inactivation, Oncogene 17 (2) (1998) 199–205, https://doi.org/10.1038/sj.onc.1201919.

[17] J.Y. Liu, G.P. Souroullas, B.O. Diekman, et al., Cells exhibiting strong p16 INK4a promoter activation in vivo display features of senescence, Proc. Natl. Acad. Sci. U.S.A. 116 (7) (2019) 2603–2611, https://doi.org/10.1073/pnas.1818313116.

[18] C.S. Tuttle, S.W. Luesken, M.E. Waaijer, A.B. Maier, Senescence in tissue samples of humans with age-related diseases: a systematic review, Ageing Res. Rev. 68 (2021), 101334, https://doi.org/10.1016/j.arr.2021.101334.

[19] W.D. Foulkes, T.Y. Flanders, P.M. Pollock, N.K. Hayward, The CDKN2A (p16) gene and human cancer, Mol. Med. 3 (1) (1997) 5–20, https://doi.org/10.1007/BF03401664.

[20] W.H. Liggett Jr., D. Sidransky, Role of the p16 tumor suppressor gene in cancer, J. Clin. Oncol. 16 (3) (1998) 1197–1206, https://doi.org/10.1200/JCO.1998.16.3.1197.

[21] J.W. Rocco, D. Sidransky, p16 (MTS-1/CDKN2/INK4a) in cancer progression, Exp. Cell Res. 264 (1) (2001) 42–55, https://doi.org/10.1006/excr.2000.5149.

[22] E.K. Yim, J.S. Park, The role of HPV E6 and E7 oncoproteins in HPV-associated cervical carcinogenesis, Cancer Res. Treat. 37 (6) (2005) 319–324, https://doi.org/10.4143/crt.2005.37.6.319.

[23] I. Lesnikova, M. Lidang, S. Hamilton-Dutoit, J. Koch, p16 as a diagnostic marker of cervical neoplasia: a tissue microarray study of 796 archival specimens, Diagn. Pathol. 4 (1) (2009) 1–7.

[24] C.W. Chia, C.A. Sherman-Baust, S.A. Larson, et al., Age-associated expression of p21and p53 during human wound healing, Aging Cell 20 (5) (2021), e13354, https://doi.org/10.1111/acel.13354.

[25] Y. Yin, G. Solomon, C. Deng, J.C. Barrett, Differential regulation of p21 by p53 and Rb in cellular response to oxidative stress, Mol. Carcinog. 24 (1) (1999) 15–24, https://doi.org/10.1002/(SICI)1098-2744, 199901)24:1<15::AID-MC3>3.0.CO;2-Y.

[26] Y.M. Kim, H.O. Byun, B.A. Jee, et al., Implications of time-series gene expression profiles of replicative senescence, Aging Cell 12 (4) (2013) 622–634, https://doi.org/10.1111/acel.12087.

[27] Q.M. Chen, J. Liu, J.B. Merrett, Apoptosis or senescence-like growth arrest: influence of cell-cycle position, p53, p21 and bax in H2O2 response of normal human fibroblasts, Biochem. J. 347 (2) (2000) 543–551, https://doi.org/10.1042/bj3470543.

[28] A.A. Elbendary, F.D. Cirisano, A.C. Evans Jr., et al., Relationship between p21 expression and mutation of the p53 tumor suppressor gene in normal and malignant ovarian epithelial cells, Clin. Cancer Res. 2 (9) (1996) 1571–1575.

[29] C. Keshava, B.L. Frye, M.S. Wolff, E.C. McCanlies, A. Weston, Waf-1 (p21) and p53 polymorphisms in breast cancer, Cancer Epidemiol. Biomark. Prev. 11 (1) (2002) 127–130.

[30] X.L. Li, J. Zhou, Z.R. Chen, W.J. Chng, P53 mutations in colorectal cancer-molecular pathogenesis and pharmacological reactivation, World J. Gastroenterol. 21 (1) (2015) 84, https://doi.org/10.3748/wjg.v21.i1.84.

[31] S. Ogino, K. Nosho, K. Shima, et al., p21 expression in colon cancer and modifying effects of patient age and body mass index on Prognosisp21, age, BMI, and prognosis in colon cancer, Cancer Epidemiol. Biomark. Prev. 18 (9) (2009) 2513–2521, https://doi.org/10.1158/1055-9965.EPI-09-0451.

[32] K.M. Aird, R. Zhang, Detection of senescence-associated heterochromatin foci (SAHF), in: L. Galluzzi, I. Vitale, O. Kepp, G. Kroemer (Eds.), Cell Senescence, Methods in Molecular Biology, vol. 965, 2013, pp. 185–196, https://doi.org/10.1007/978-1-62703-239-1_12.

[33] F. Uhlitz, P. Bischoff, S. Peidli, et al., Mitogen-activated protein kinase activity drives cell trajectories in colorectal cancer, EMBO Mol. Med. 13 (10) (2021), e14123, https://doi.org/10.15252/emmm.202114123.

[34] Y. Hao, S. Hao, E. Andersen-Nissen, et al., Integrated analysis of multiodal single-cell data, Cell 184 (13) (2021) 3573–3587, https://doi.org/10.1016/j.cell.2021.04.048.

[35] G. Korotkevich, V. Sukhov, A. Sergushichev, Fast Gene Set Enrichment Analysis, bioRxiv, 2019, https://doi.org/10.1101/060012. http://biorxiv.org/content/early/2016/06/20/060012.

[36] A. Subramanian, P. Tamayo, V.K. Mootha, et al., Gene set enrichment analysis: a knowledge-based approach for interpreting genome-wide expression profiles, Proc. Natl. Acad. Sci. U.S.A. 102 (43) (2005) 15545–15550, https://doi.org/10.1073/pnas.0506580102.

[37] A.L. Fridman, M.A. Tainsky, Critical pathways in cellular senescence and immortalization revealed by gene expression profiling, Oncogene 27 (46) (2008) 5975–5987, https://doi.org/10.1038/onc.2008.213.

[38] O. Pluquet, C. Abbadie, O. Coqueret, Connecting cancer relapse with senescence, Cancer Lett. 463 (2019) 50–58, https://doi.org/10.1016/j.canlet.2019.08.004.

[39] M. Demaria, M.N. O'Leary, J. Chang, et al., Cellular senescence promotes adverse effects of chemotherapy and cancer RelapseCellular senescence and chemotherapy, Cancer Discov. 7 (2) (2017) 165–176.

[40] J.M. Flores, J. Martín-Caballero, R.A. García-Fernández, p21 and p27 a shared senescence history, Cell Cycle 13 (11) (2014) 1655–1656, https://doi.org/10.4161/cc.29147.

[41] N. Kapranos, G.P. Stathopoulos, L. Manolopoulos, et al., p53, p21 and p27 protein expression in head and neck cancer and their prognostic value, Anticancer Res. 21 (1B) (2001) 521–528.
[42] Y.H. Seo, Y.E. Joo, S.K. Choi, J.S. Rew, C.S. Park, S.J. Kim, Prognostic significance of p21 and p53 expression in gastric cancer, Korean J. Intern. Med. 18 (2) (2003) 98, https://doi.org/10.3904/kjim.2003.18.2.98.
[43] K. Engeland, Cell cycle regulation: p53-p21-RB signaling, Cell Death Differ. 29 (5) (2022) 946–960, https://doi.org/10.1038/s41418-022-00988-z.
[44] B.Y. Lee, J.A. Han, J.S. Im, et al., Senescence-associated β-galactosidase is lysosomal β-galactosidase, Aging Cell 5 (2) (2006) 187–195, https://doi.org/10.1111/j.1474-9726.2006.00199.x.
[45] J. Zhang, Y. Wang, Y. Shen, P. He, J. Ding, Y. Chen, G9a stimulates CRC growth by inducing p53 Lys373 dimethylation-dependent activation of Plk1, Theranostics 8 (10) (2018) 2884–2895, https://doi.org/10.7150/thno.23824.
[46] N.A. Barlev, L. Liu, N.H. Chehab, et al., Acetylation of p53 activates transcription through recruitment of coactivators/histone acetyltransferases, Mol. Cell 8 (6) (2001) 1243–1254, https://doi.org/10.1016/S1097-2765(01)00414-2.
[47] M. Ocker, S. Al Bitar, A.C. Monteiro, H. Gali-Muhtasib, R. Schneider-Stock, Epigenetic regulation of p21cip1/waf1 in human cancer, Cancers 11 (9) (2019) 1343, https://doi.org/10.3390/cancers11091343.
[48] J. Campisi, Senescent cells, tumor suppression, and organismal aging: good citizens, bad neighbors, Cell 120 (4) (2005) 513–522, https://doi.org/10.1016/j.cell.2005.02.003.
[49] A. Kapić, H. Helmbold, R. Reimer, O. Klotzsche, W. Deppert, W. Bohn, Cooperation between p53 and p130(Rb2) in induction of cellular senescence, Cell Death Differ. 13 (2) (2006) 324–334, https://doi.org/10.1038/sj.cdd.4401756.
[50] H. Helmbold, N. Kömm, W. Deppert, W. Bohn, Rb2/p130 is the dominating pocket protein in the p53–p21 DNA damage response pathway leading to senescence, Oncogene 28 (39) (2009) 3456–3467, https://doi.org/10.1038/onc.2009.222.
[51] H. Rayess, M.B. Wang, E.S. Srivatsan, Cellular senescence and tumor suppressor gene p16, Int. J. Cancer 130 (8) (2012) 1715–1725, https://doi.org/10.1002/ijc.27316.
[52] C.M. Beauséjour, A. Krtolica, F. Galimi, et al., Reversal of human cellular senescence: roles of p53 and p16 pathways, EMBO J. 22 (16) (2003) 4212–4222, https://doi.org/10.1093/emboj/cdg417.
[53] H. Kitamura, H. Takemura, T. Minamoto, Tumor p16INK4 gene expression and prognosis in colorectal cancer, Oncol. Rep. 41 (2) (2019) 1367–1376, https://doi.org/10.3892/or.2018.6884.
[54] K. Shima, K. Nosho, Y. Baba, et al., Prognostic significance of CDKN2A (p16) promoter methylation and loss of expression in 902 colorectal cancers: cohort study and literature review, Int. J. Cancer 128 (5) (2011) 1080–1094, https://doi.org/10.1002/ijc.25432.
[55] P. Krimpenfort, A. Ijpenberg, J.Y. Song, et al., p15Ink4b is a critical tumour suppressor in the absence of p16Ink4a, Nature 448 (7156) (2007) 943–946, https://doi.org/10.1038/nature06084.
[56] M. Storer, A. Mas, A. Robert-Moreno, et al., Senescence is a developmental mechanism that contributes to embryonic growth and patterning, Cell 155 (5) (2013) 1119–1130, https://doi.org/10.1016/j.cell.2013.10.041.
[57] R. Kumari, P. Jat, Mechanisms of cellular senescence: cell cycle arrest and senescence associated secretory phenotype, Front. Cell Dev. Biol. 9 (2021), 645593, https://doi.org/10.3389/fcell.2021.645593.
[58] K. Mirzakhani, J. Kallenbach, S.M. Rasa, et al., The androgen receptor—lncRNASAT1-AKT-p15 axis mediates androgen-induced cellular senescence in prostate cancer cells, Oncogene 41 (7) (2022) 943–959, https://doi.org/10.1038/s41388-021-02060-5.
[59] D.S. Markowitz, M.M. Bertagnolli, Molecular basis of colorectal cancer, N. Engl. J. Med. 361 (25) (2009) 2449–2460, https://doi.org/10.1056/NEJMra0804588.
[60] T. Kuilman, C. Michaloglou, L.C. Vredeveld, et al., Oncogene-induced senescence relayed by an interleukin-dependent inflammatory network, Cell 133 (6) (2008) 1019–1031, https://doi.org/10.1016/j.cell.2008.03.039.
[61] Y.I. Li, C.D. de Haar, M. Chen, et al., Disease-related expression of the IL6/STAT3/SOCS3 signalling pathway in ulcerative colitis and ulcerative colitis-related carcinogenesis, Gut 59 (2) (2010) 227–235, https://doi.org/10.1136/gut.2009.206938.
[62] X.L. Liu, J. Ding, L.H. Meng, Oncogene-induced senescence: a double edged sword in cancer, Acta Pharmacol. Sin. 39 (10) (2018) 1553–1558, https://doi.org/10.1038/aps.2017.198.
[63] K. Yoshimoto, C. Tanaka, S. Yamada, et al., Infrequent mutations of p16INK4A and p15INK4B genes in human pituitary adenomas, Eur. J. Endocrinol. 136 (1) (1997) 74–80, https://doi.org/10.1530/eje.0.1360074.
[64] S. Yoshida, T. Todoroki, Y. Ichikawa, et al., Mutations of p16INK4/CDKN2 and p15 INK4B/MTS2 genes in biliary tract cancers, Cancer Res. 55 (13) (1995) 2756–2760.
[65] E.P. Xing, Y. Nie, Y. Song, et al., Mechanisms of inactivation of p14 ARF, p15 INK4b, and p16 INK4a genes in human esophageal squamous cell carcinoma, Clin. Cancer Res. 5 (10) (1999) 2704–2713.
[66] Q. Tu, J. Hao, X. Zhou, et al., CDKN2B deletion is essential for pancreatic cancer development instead of unmeaningful co-deletion due to juxtaposition to CDKN2A, Oncogene 37 (1) (2018) 128–138, https://doi.org/10.1038/onc.2017.316.
[67] H. Suzuki, X. Zhou, J. Yin, et al., Intragenic mutations of CDKN2B and CDKN2A in primary human esophageal cancers, Hum. Mol. Genet. 4 (10) (1995) 1883–1887, https://doi.org/10.1093/hmg/4.10.1883.
[68] W. Jang, J. Park, A. Kwon, et al., CDKN2B downregulation and other genetic characteristics in T-acute lymphoblastic leukemia, Exp. Mol. Med. 51 (1) (2019) 1–15, https://doi.org/10.1038/s12276-018-0195-x.
[69] Y. Xia, Y. Liu, C. Yang, et al., Dominant role of CDKN2B/p15INK4B of 9p21.3 tumor suppressor hub in inhibition of cell-cycle and glycolysis, Nat. Commun. 12 (1) (2021), https://doi.org/10.1038/s41467-021-22327-5, 2047.